

Graph-based many-to-one dynamic ride-matching for shared mobility services on congested networks

Seyed Mehdi Meshkani^{a,*}, Bilal Farooq^a

^a*Laboratory of Innovations in Transportation (LiTrans), Ryerson University, Canada*

Abstract

On-demand shared mobility systems require matching of one (one-to-one) or multiple riders (many-to-one) to a vehicle based on real-time information. We propose a novel Graph-based Many-to-One ride-Matching (GMOMatch) algorithm for the dynamic many-to-one matching problem in the presence of traffic congestion. The proposed algorithm, which is an iterative two-step method, provides high service quality and is efficient in terms of computational complexity. GMOMatch starts with a one-to-one matching in Step 1 and is followed by solving a maximum weight matching problem in Step 2 to combine the travel requests. To evaluate the performance of the proposed algorithm, it is compared with a ride-matching algorithm developed by IBM (Simonetto et al., 2019). Both algorithms are implemented in a micro-traffic simulator to assess their performance and their impact on traffic congestion. Downtown Toronto road network was chosen as the study area. In comparison to the IBM algorithm, GMOMatch improved the service quality and traffic travel time by 32% and 4%, respectively. The sensitivity analysis indicated that in downtown Toronto, utilizing vehicles with a capacity of 10, can achieve 25% improvement in comparison to a capacity of 4, which also meant a lower fleet size on the network.

Keywords: Shared on-demand mobility, ride-matching, graph-based algorithm, congested network

1. Introduction

According to the United Nations (UN), 68% of the world's population will live in urban areas by 2050 (Ritchie, 2018). Such rapid growth in urbanization increases the demand for transportation (Tafreshian and Masoud, 2020). To simultaneously satisfy this demand and alleviate the negative impacts of transportation (e.g, road congestion and emissions), more sustainable forms of travel modes need to be conceived. Over the past few years, with the advancements in information and communication technology, emergence of smartphones, and ubiquity of high-speed internet, on-demand shared mobility services such as ridehailing and ridesharing as more sustainable forms of transportation have gained attention and have shown considerable growth in recent years (Agatz et al., 2011; Feng et al., 2017). Benefits of such modes include a point-to-point high level of service, decrease in traffic congestion and emissions, decline in parking space demand, and reduction in travel cost (Mourad et al., 2019; Najmi et al., 2017). However, a study conducted by Castiglione et al. (2018) to evaluate the traffic congestion in San Francisco between 2010 and 2016 showed that on-demand transportation companies such as Uber and Lyft contribute significantly to the increase in traffic congestion. To obtain sustainable benefits from such on-demand services, well-designed systems need to be developed that can utilize the supply optimally, while providing a high level of service.

The ride-matching problem as the core of ridehailing and ridesharing systems is the generalization of the dial-a-ride problem (DARP) that finds the best vehicle from a large pool of vehicles for a ride request (Yu et al., 2019; Tafreshian et al., 2020). Many-to-one dynamic ride-matching is needed in the on-demand shared mobility services, where one vehicle can serve multiple riders simultaneously. According

*Corresponding Author.

Email addresses: smeshkani@ryerson.ca (Seyed Mehdi Meshkani), bilal.farooq@ryerson.ca (Bilal Farooq)

to [Lokhandwala and Cai \(2018\)](#), with an increase in the vehicle occupancy rate due to ridesharing, the current taxi fleet can be reduced by 59%, while maintaining the service quality. Various studies have addressed the many-to-one ride-matching problem ([Masoud and Jayakrishnan, 2017b](#); [Alonso-Mora et al., 2017](#); [Simonetto et al., 2019](#); [Tafreshian and Masoud, 2020](#)). Computational complexity and service quality are two important aspects of such problems. [Masoud and Jayakrishnan \(2017b\)](#) utilized the first-come, first-serve (FCFS) strategy to match riders with the vehicles. Although FCFS is efficient in terms of computational complexity, there is no guarantee to provide a ride-matching system with a high-quality level of service, especially in congested networks. [Alonso-Mora et al. \(2017\)](#) developed a multi-step algorithm for the many-to-one ride-matching problem, which provided high service quality. However, the proposed algorithm used a heuristic method to solve an integer optimization problem that may face scalability issues. [Simonetto et al. \(2019\)](#) proposed a ride-matching method based on the linear assignment problem. The method is computationally efficient. However, in each iteration, only a one-to-one matching problem is solved, and riders are not combined. In such a strategy, the quality of the service can not always be guaranteed. [Tafreshian and Masoud \(2020\)](#) proposed a many-to-one ridesharing algorithm based on the graph partitioning method. Although the algorithm has been shown to be computationally efficient on small-scale, the resulting high number of clusters in large-scale problems is expected to affect the algorithm's performance negatively. The algorithm was only demonstrated on low capacity vehicles (3 passengers). Due to the need for higher number of clusters, it is expected that the performance of the algorithm will deteriorate when medium/high capacity vehicles are in the mix.

In this work, we propose a novel graph-based heuristic algorithm for the dynamic many-to-one ride-matching problem that reduces the computational complexity of the problem, while providing high-quality service in a congested network. The proposed Graph-based Many-to-One ride-Matching (GMO-Match) algorithm is iterative and consists of two steps. In the first step, riders are assigned to vehicles by solving a one-to-one ride-matching problem. In the second step, a maximum weight matching problem is solved to combine riders with similar itineraries through the idea of matching vehicles. Furthermore, the proposed algorithm is implemented on an agent-based micro-traffic simulator to measure different indicators and examine the impact of ride-matching algorithm on traffic congestion. Finally, to evaluate our algorithm's performance, a comparison is conducted with the matching algorithm developed by [Simonetto et al. \(2019\)](#) at IBM. The GMOMatch ride-matching algorithm can be used in different types of shared mobility services (static/dynamic) such as ridehailing, ridesharing, microtransit, and shuttles.

The rest of this paper is organized as follows. In Section 2, we briefly review the relevant literature on ridehailing and ridesharing services. Section 3 introduces the dynamic ride-matching system, including system setting, system framework, and details of the ride-matching algorithm (GMOMatch). Section 4 presents the description of the case study, results and discussions. Finally, Section 5 concludes our findings and provides some directions for future research.

2. Background

Dynamic ridehailing and ridesharing are the two common types of on-demand shared mobility services. Dynamic ridehailing is a transportation service for compensation in which drivers and passengers are matched in real-time ([Shaheen et al., 2019](#)). In such systems, drivers unlike passengers do not have a tight time window ([Tafreshian et al., 2020](#)), which makes it more similar to a taxi service. Dynamic ridesharing is a service that connects drivers and passengers with similar itineraries and time schedules in order to split travel costs ([Agatz et al., 2011](#); [Shaheen et al., 2019](#)). In both systems, drivers and passengers are connected by a mobility service provider, mostly through a mobile application based on real-time information ([Agatz et al., 2012](#); [Shaheen et al., 2019](#); [Wang and Yang, 2019](#)).

Ridehailing and ridesharing systems in the literature can be characterized by various features such as matching type and modelling scale. Some research efforts in the literature focused on the one-to-one matching problem in which a single driver/ vehicle can be matched with at most one rider ([Agatz et al., 2011](#); [Nourinejad and Roorda, 2016](#); [Najmi et al., 2017](#); [Lyu et al., 2019](#); [Bertsimas et al., 2019](#); [Özkan and Ward, 2020](#)). Other studies addressed the many-to-one matching problem where a single vehi-

cle/driver serves multiple riders (Jung et al., 2016; Alonso-Mora et al., 2017; Masoud and Jayakrishnan, 2017a,b; Qian et al., 2017; Simonetto et al., 2019).

Jung et al. (2016) introduced a Hybrid-Simulated Annealing (HSA) algorithm to solve the dynamic ride-matching problem. They used Korea Transport Institute (KOTI) regional transportation planning model to simulate their proposed algorithm. Their results revealed that HSA can enhance the efficiency of dynamic ridesharing systems. Masoud and Jayakrishnan (2017a) proposed a decomposition algorithm to convert the original many-to-many ride-matching problem into smaller sub-problems that are tractable computationally. They introduced a pre-processing procedure to reduce the size of the optimization problem. Sub-problems are independent from each other which allows computations to be done in parallel. To evaluate the performance of the decomposition algorithm, they generated 420 random instances, with each instance different in terms of the number of riders and drivers. They applied it on a grid network with 49 pickup/dropoff stations, where the number of participants varied between 20-400. The earliest departure times of all trips were generated randomly within a one-hour time period. Also, in another research effort, Masoud and Jayakrishnan (2017b) presented a real-time and optimal algorithm for many-to-many ride-matching problem, which aimed to maximize the number of served rider in the system. Their matching algorithm was based on FCFS, while the participant itineraries are determined using the dynamic programming. To improve the quality of the solution obtained by FCFS, they introduced a peer-to-peer exchange method. To assess the performance of the algorithm, they generated multiple random instances of ridesharing problem with different ratio of riders to drivers. The size of the participants was 1000. Similar to the previous study, they used a grid network with 59 stations and randomly generated the trips within a one-hour time period. Qian et al. (2017) addressed the taxi group ride problem (TGR) to optimally grouping passengers with similar itineraries. They proposed three algorithms, including exact, heuristic, and greedy algorithms. To evaluate the performance of the algorithm, they used the taxi trajectory datasets from New York City (NYC), Wuhan, and Shenzhen. Their results showed that the heuristic outperformed the exact and greedy algorithms in terms of computational efficiency and solution quality.

Alonso-Mora et al. (2017) proposed a multi-step graph-based procedure to assign drivers to riders efficiently. Their algorithm allowed the use of low as well as high capacity vehicles. First, they created a shareability graph of requests and vehicles. Next, the graph of candidate trips, and vehicles that can execute them is created. Finally, using integer linear programming (ILP), they optimally assign requests to vehicles. The computational complexity of ILP is $O(mn^v)$, where m is the number of vehicles, n is the number of requests, and v is the maximum capacity of the vehicles. They used NYC taxi data to evaluate the performance of their algorithm. Their results showed that 98% of the taxi rides could be served with just 3,000 taxis with a capacity four, instead of the existing 13,000 taxis. Simonetto et al. (2019) used a federated architecture to linearly assign requests to vehicles. The proposed system consisted of a context-mapping algorithm to filter vehicles, a single dial-a-ride problem to obtain optimal travel route and associated cost, and a linear assignment problem to optimally match requests to vehicles. They used the NYC and Melbourne Metropolitan Area datasets to evaluate the system performance. They compared their algorithm with Alonso-Mora et al. (2017) and reported less computational complexity, while maintaining high-quality ride-matching level of service. Tafreshian and Masoud (2020) proposed a graph partitioning method for the one-to-one matching problem in bipartite graphs. It is then extended to a more complex case, where one vehicle can serve multiple riders (many-to-one matching). However, the computational complexity of such problem increased and an exhaustive evaluation was not practical. Thus, only two scenarios with a vehicle capacity of three were evaluated. Furthermore, using a high number of clusters in large size problems may adversely affect the performance.

Another dimension of ridehailing and ridesharing systems in the literature is the modelling scale. Most of the studies in the context of ridehailing and ridesharing have been simulated and implemented at macroscopic/mesoscopic scale (Nourinejad and Roorda, 2016; Masoud and Jayakrishnan, 2017a; Alonso-Mora et al., 2017; Simonetto et al., 2019; Tafreshian and Masoud, 2020). One of the issues associated with these scales is that it is not clear how the proposed ride-matching system and traffic congestion affect each other in the presence of other vehicles (Gu  riaux et al., 2020). Some recent studies

in the context of shared automated vehicles (SAVs) used microsimulation to address how SAVs affects urban mobility systems (Dandl et al., 2017; Oh et al., 2020; Huang et al., 2020; Guériau et al., 2020). Dandl et al. (2017) deployed a microsimulation model to study how an autonomous taxi system affected the traffic network in the city of Munich. Oh et al. (2020) assessed the performance of shared driverless taxis including demand, supply and their interactions. On the supply side, they developed a heuristic matching and routing algorithm. Huang et al. (2020) explored the idea of using the SAVs to bring first-mile last-mile connectivity to transit in automated mobility districts. Guériau et al. (2020) developed a reinforcement learning-based shared autonomous mobility on-demand system with dynamic ridesharing and rebalancing strategies where vehicles consider traffic congestion in their decisions.

Table 1 summarizes the major features of the recent literature on the ride-matching problem. Some studies in the literature, for instance, Masoud and Jayakrishnan (2017a) and Tafreshian and Masoud (2020), utilized decomposition or partitioning methods to convert the problem into several sub-problems. On the other hand, our proposed algorithm is in the class of algorithms that formulates the problem centrally and has access to the entire information of the ride-matching system. Alonso-Mora et al. (2017) and Simonetto et al. (2019) are some of the recent examples of such a class. Masoud and Jayakrishnan (2017b) utilized the FCFS strategy for matching, which may not be an appropriate approach for a congested network. We consider the entire batch of requests and match them simultaneously, which enhances the quality of the matching and consequently system performance. In Alonso-Mora et al. (2017), the computational complexity is dependent on the vehicle capacity, which may cause the scalability issue. The computational complexity of the proposed algorithm is fixed and is the same as that of the IBM algorithm by Simonetto et al. (2019). Nevertheless, unlike Simonetto et al. (2019), where each vehicle is matched with only one rider at each update time, our algorithm combines requests with similar itineraries, leading to utilizing the available vehicles more efficiently, improving the quality of service, and enhancing the traffic congestion. Table 1 indicates that most of the studies considered a macro/mesoscopic approach for the ride-matching problem and there are only a few studies that utilize microscopic scale to develop a ride-matching system. However, in those cases, developing a new ride-matching algorithm that considered and improved the complexity and service quality of the problem was not the main contribution. In this paper, we introduce a novel many-to-one ride-matching algorithm for the dynamic on demand shared mobility in the congested networks, which aims to improve the service quality, while considering the computational complexity. We deploy a micro-traffic simulator to examine the algorithm’s performance on the service quality and network traffic.

Table 1: Literature on ride-matching problem

| Study | Matching type | | Assignment | | Modeling scale | |
|--------------------------------|---------------|-------------|-------------|---------------------------|------------------|-------------|
| | one-to-one | many-to-one | centralized | decomposing /partitioning | macro/mesoscopic | microscopic |
| Agatz et al., 2011 | * | | * | | * | |
| Nourinejad and Roorda, 2016 | * | | | * | * | |
| Najmi et al., 2017 | * | | | * | * | |
| Lyu et al., 2019 | * | | * | | * | |
| Bertsimas et al., 2019 | * | | * | | * | |
| Özkan and Ward, 2020 | * | | * | | * | |
| Jung et al., 2016 | | * | * | | * | |
| Alonso-Mora et al., 2017 | | * | * | | * | |
| Masoud and Jayakrishnan, 2017a | | * | | * | * | |
| Masoud and Jayakrishnan, 2017b | | * | * | | * | |
| Qian et al., 2017 | | * | * | | * | |
| Simonetto et al., 2019 | | * | * | | * | |
| Tafreshian and Masoud, 2020 | | * | | * | * | |
| Oh et al., 2020 | * | | * | | | * |
| Guériau et al., 2020 | | * | | * | | * |
| This study | | * | * | | | * |

3. Methodology

In the many-to-one ride-matching problem, one vehicle can serve multiple riders, while one rider can only be served by a single vehicle. This problem is a special case of general pick-up and delivery problem introduced by [Savelsbergh and Sol \(1995\)](#), and is known to be NP-hard ([Qian et al., 2017](#); [Tafreshian and Masoud, 2020](#)). Therefore, for large-scale dynamic ride-matching problems, it is not practical to use exact methods to solve the problem in a short period of time. Thus, heuristic algorithms are proposed to solve this problem efficiently for large instances. In this section, we first introduce the general setup of a dynamic ride-matching system and its characteristics. We then propose the heuristic dynamic many-to-one ride-matching algorithm.

3.1. Dynamic ride-matching system setup

We consider a set of ride requests $R = \{r_1, r_2, \dots, r_n\}$ and a set of vehicles $V = \{v_1, v_2, \dots, v_j\}$ with total capacity of cap at time t . The ride-matching service aims to assign online ride requests to vehicles and find corresponding schedules while some constraints are satisfied. A ride request/rider refers to a person who places his/her order mostly through a mobile application to be picked up from his origin and to be dropped off at his destination. An available vehicle is a vehicle that has at least one empty seat. Each available vehicle can be assigned no more than its current empty seats. Furthermore, a passenger refers to a ride request that has been assigned to a vehicle. This passenger can be already on-board or can be waiting to be picked up. The set of passengers assigned to a vehicle $v \in V$ is denoted by P_v .

Each request $r \in R$ consists of a request-time (t_r), origin (O_r), and destination (D_r). In addition, as in [Agatz et al. \(2011\)](#), we assume that each request (r) provides an earliest departure time from their origin (e_r) and latest time they would like to arrive at their destination (l_r) (see Fig. 1a). Furthermore, there is time flexibility which specifies the difference between rider's earliest departure time and the latest time (q_r) he would like to depart and is computed as $f_r = l_r - e_r - T(O_r, D_r)$, where $T(O_r, D_r)$ is the travel time when rider directly goes from his origin to destination. Without the loss of generality in order to make the system more dynamic, in this study, we assume that travel request time and their earliest departure time are the same ($t_r = e_r$).

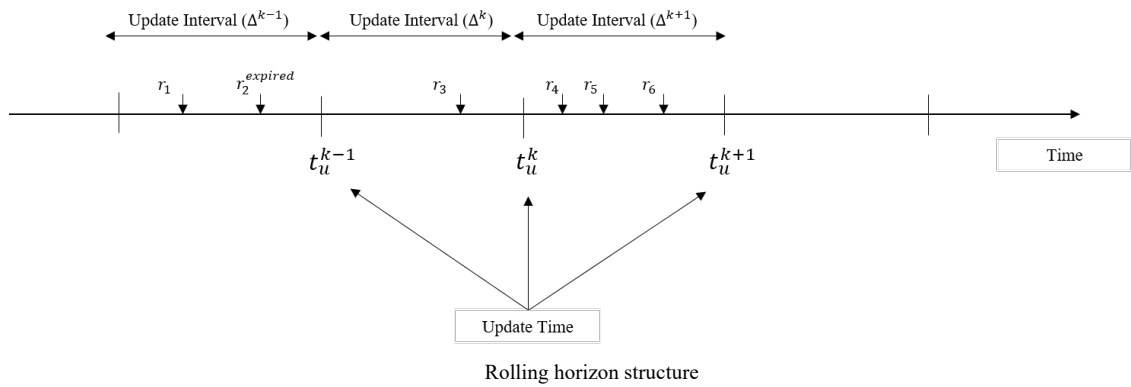
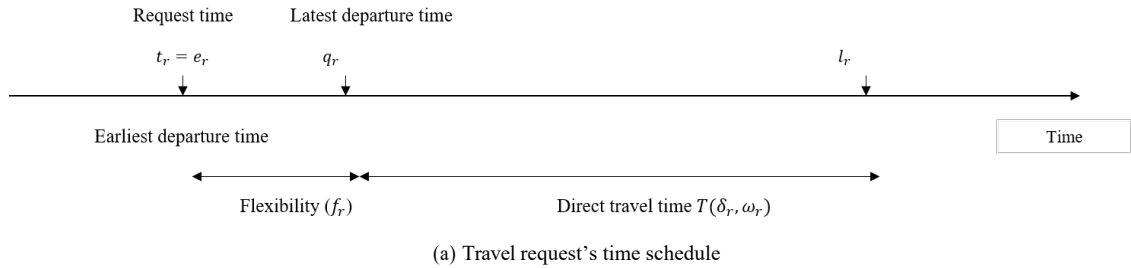


Figure 1: Ride-matching system setting

To solve the dynamic ride-matching problem in real time, we use the rolling horizon strategy suggested by Agatz et al. (2011). In this strategy, the ride-matching algorithm is solved periodically at specific time over fixed time intervals referred to as “update time” $t_u^k (k = 0, 1, 2, \dots)$ and update interval $(\Delta^k = t_u^k - t_u^{k-1})$ (see Fig. 1b). During each update interval, new riders place their orders to get a ride. At each update time, the system operator considers both new riders and those who have not been finalized or expired. A request is finalized when assigned to a vehicle and is expired when the current time exceeds the request’s latest departure time while it has not been assigned to a vehicle yet. Rolling horizon iterations continue until all riders exit the system either by being matching or by having expired. As an example, in Fig. 1b, when the system operator runs the ride-matching algorithm at current time t_u^{k+1} , it includes all of the new requests $\{r_4, r_5, r_6\}$ over update interval Δ^{k+1} and all requests $\{r_1, r_3\}$ related to previous update intervals Δ^k and Δ^{k-1} but r_2 which has been expired because the current time t_u^{k+1} exceeds r_2 ’s latest departure time.

A set of constraints Z consists of a capacity constraint (z_0) and two time constraints (z_1, z_2). These constraints need to be satisfied so that one vehicle potentially is capable of serving a request. The zero constraint z_0 ensures that each vehicle has at least one empty space. In other words, zero constraint finds available vehicles. The first constraint (z_1) states that any request r should be picked up no longer than its latest departure time q_r and the second constraint (z_2) expresses that it should be dropped off no longer than its latest departure time l_r .

3.2. GMOMatch algorithm

Given a set of ride requests R and set of vehicles V at current time t from section 3.1, the many-to-one ride-matching problem is the matching of riders with vehicles such that each vehicle can be matched with multiple riders. In this problem vehicles can be low, medium, or high capacity. To solve this problem, we propose the GMOMatch which is a graph-based iterative algorithm that returns requests-vehicles matching and pick up/drop off scheduling. Fig. 2 illustrates the GMOMatch algorithm along with a simple example.

The algorithm consists of two steps (Fig. 2a). In the first step, we consider a bipartite graph to match requests with vehicles. Vehicles can be idle or enroute. The output of this step is one-to-one matching and creating a set of assigned vehicles (Definition 1). In the second step which is iterative, we create a vehicle directed graph whose vertices are assigned vehicles. We then solve a maximum weight matching problem to match assigned vehicles with each other (Definition 2) and combine associated requests. The main algorithm is also iterative and ends when some criteria are satisfied. We are assuming that the shared mobility service has a routing agent that can calculate the optimal path between two locations on a network using existing or predicted traffic conditions. This is a practical assumption, given the current level of sensorization in dense urban areas and the amount of probe vehicles on the network.

Definition 1: Let R_v be the assigned requests set, which is the set of requests assigned to vehicle v during the matching process. It is empty at the beginning of the matching at every update time $t_u^k (\forall v \in V : R_v = \emptyset)$. A vehicle $v \in V$ is defined as an assigned vehicle if its requests set is not empty ($R_v \neq \emptyset$). As an example in Fig. 3 (a) both vehicles v_n and v_n are assigned vehicles while in 3 (b) just v_n is considered assigned vehicle.

Definition 2: Two assigned vehicles v_n and v_n are matched with each other when requests set of one of them depending on the direction of link between them is assigned to the other one. As presented in Fig. 3, vehicle v_n is matched with vehicle v_n (a) which means that its requests set is assigned to v_n (b).

Figures 2b and 2c show a small example of how the GMOMatch algorithm works to assign requests to vehicles. In Fig. 2b, there are a set of requests and vehicles. The algorithm starts with solving a one-to-one matching problem in step 1 and assigns four requests (out of eight) to four vehicles. In the first iteration of step 2, by solving a maximum weight matching problem, vehicle 3 is matched with vehicle 2 which leads to combining requests 3 and 7 together in the vehicle 2. Similarly, in the second iteration of step 2, vehicle 1 is matched with vehicle 2 and its associate travel request 2 is combined with requests 7 and 3 in vehicle 2. Step 2 stops until some criteria are satisfied. Since four non-assigned requests are still left, the algorithm needs to move toward the second iteration (Fig. 2c). In step 1 of the

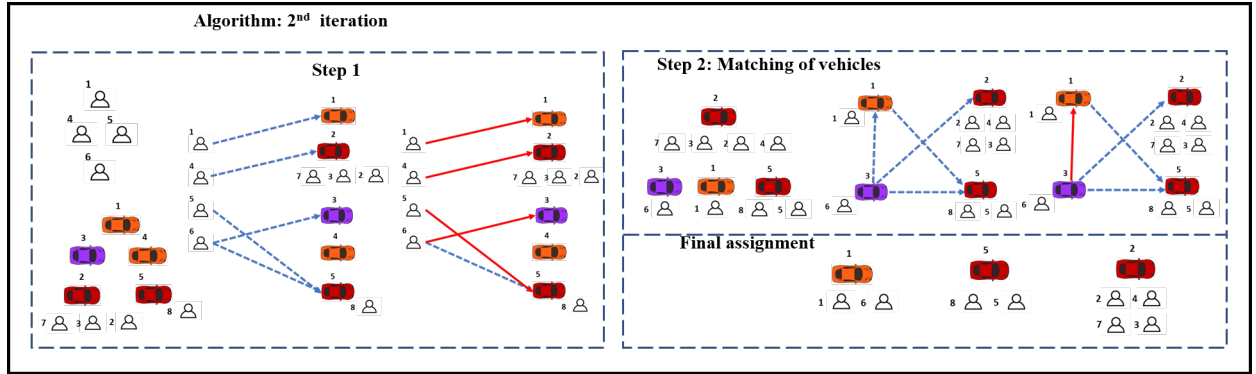
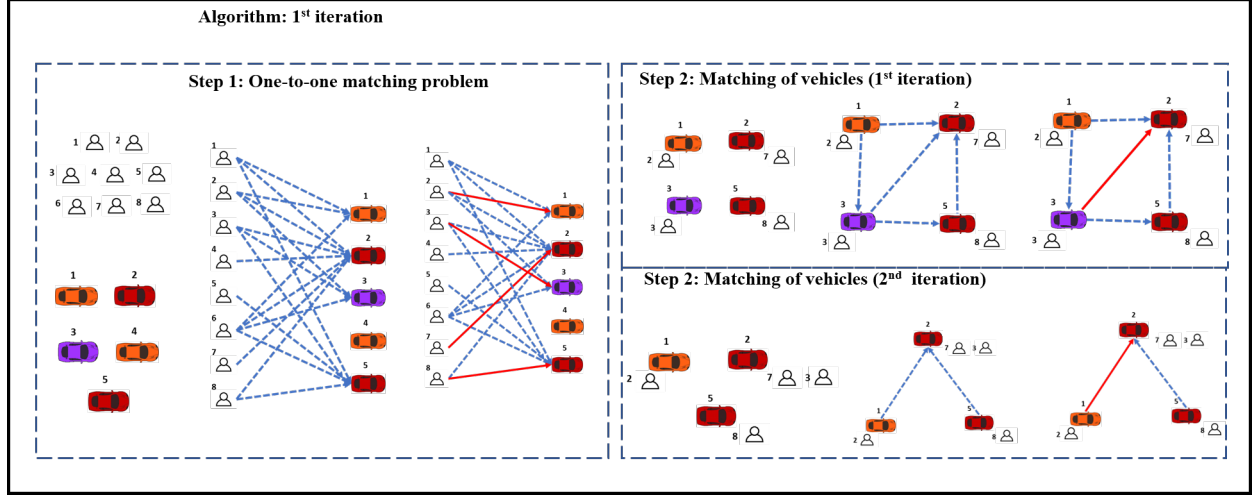
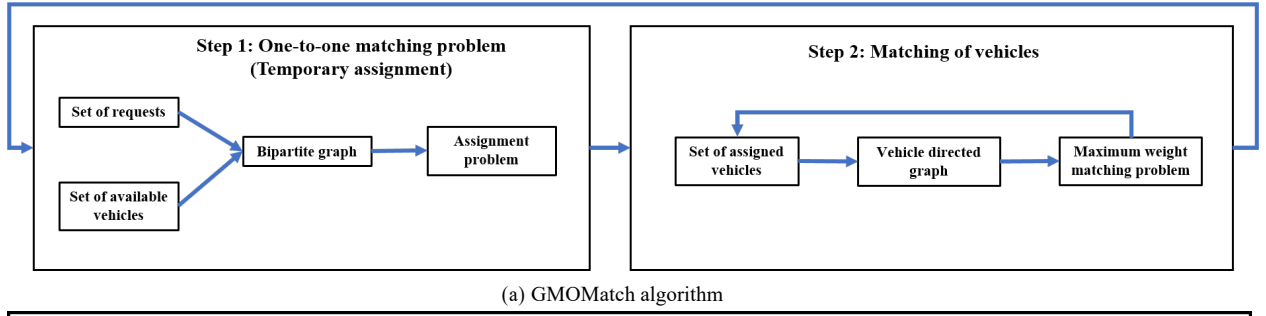


Figure 2: Two-step iterative method

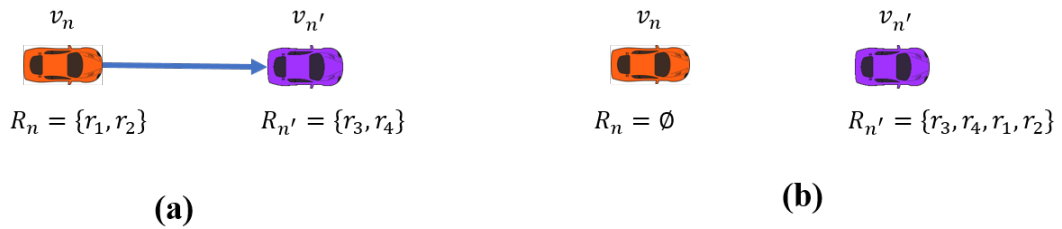


Figure 3: Matching of vehicles

second iteration, the same set of vehicles is considered and the remaining requests (four requests) assign to them. Finally, in step 2 of the second iteration, vehicle 3 is matched with vehicle 1, and requests 1 and 6 are combined in vehicle 1. Likewise, the algorithm continues until some criteria and constraints

are met. In the following, the two steps of the GMOMatch algorithm will be explained in detail.

3.3. Step 1: one-to-one matching problem

The first step of the method is one-to-one matching problem, which can be represented by a bipartite graph $G = (I, L)$, where I is the set of nodes, including all requests and vehicles ($I = \mathcal{R} \cup V$), and L is the set of links. Link $l_{rv} \in L$ between request r and vehicle v exists if constraint set Z is satisfied. Each link has a travel cost ($c_{rv} \in C$) where C is the set of travel costs and (c_{rv}) is defined as the time duration needed by a vehicle v to serve both its already scheduled passengers and request r . The goal of the proposed one-to-one matching problem is minimizing vehicles' total travel time.

Let M be the current location of vehicle v , then z_1 and z_2 can be expressed mathematically as Eq. 1 and Eq. 2.

$$t + t_{rv}(M, O_r) \leq q_r \quad (1)$$

$$t + t_{rv}(M, O_r) + t_{rv}(O_r, D_r) \leq l_r \quad (2)$$

Where t is current time and equals update time $t = t_u^k$, $t_{rv}(M, O_r)$ is travel time from vehicle's current position to request's origin, and $t_{rv}(O_r, D_r)$ is travel time between request's origin and destination. As mentioned, Eq. 1 ensures that request r would be picked up by vehicle v no more than his latest departure time (q_r) and Eq. 2 expresses that request r would be dropped off no more than its latest arrival time (l_r).

To create a bipartite graph G , first, we specify the set of vehicles that can potentially serve each request ($V_r \subseteq V \forall r \in \mathcal{R}$) and we name it the set of feasible vehicles for request r . To this end, for each travel request r , a search space based on his time flexibility is created. By assuming request r is the first passenger to be picked up, all of the vehicles whose travel time from their current location to the request's origin are not more than the request's flexibility are considered (Eq. 3). Vehicles can be idle or enroute. A vehicle is enroute if it has already been assigned to some passengers and is traveling to pick up/drop off them. It is worth mentioning that creating search space for the requests can significantly reduce the problem's computational complexity. Given m number of requests and n number of vehicles, to calculate travel time the worst case is that for each request we consider all vehicles that is $O(mn)$ which scales linearly with the number of vehicles and requests. However, creating search space reduces the number of feasible vehicles significantly. Let k be the maximum number of feasible vehicles which is much less than number of vehicles $k \ll n$. In this case, the computational complexity would be $O(mk)$.

$$t_{rv}(M, O_r) \leq f_r \quad (3)$$

Proposition 1: Vehicles that violate Eq. 3 (e.g. $t_{rv}(M, O_r) > f_r$) cannot serve request r .

Proof: Based on z_1 we have the inequality $t + t_{rv}(M, O_r) \leq q_r$. On the other hand, for each request r and vehicle v , $z_2 \leq e_r$ and $t_{rv}(M, O_r) \leq f_r$. Thus, $t + t_{rv}(M, O_r) \leq e_r + f_r = q_r$ which shows z_1 is not satisfied and vehicle v cannot serve request r .

After finding vehicles for each request, their travel cost and optimal travel path is calculated. Each vehicle $v \in V$ has a current travel path (before considering request r) denoted by Λ_v and updated travel path (with considering request r) denoted by Λ_v^t , that specifies which locations need to be visited to pick up/drop off. As mentioned, the travel cost of request r ($c_{rv} \in C$) is the time duration of travel path (Λ_v^t) of vehicle v to serve its existing scheduled passengers as well as request r .

To obtain travel cost c_{rv} and optimal travel path Λ_v^t , a vehicle routing problem, which in the literature is known as a single-vehicle dial-a-ride problem (Häme, 2011; Liu et al., 2015; Ho et al., 2018), needs to be solved. The objective is to minimize the travelled path time of vehicle v subject to the constraint set Z . To do so, we propose a function whose inputs are spatiotemporal information of request r (Ω_r) (e.g. origin, destination, time window), current travel path (Λ_v) of vehicle v , spatiotemporal information of already scheduled passengers P_v (Θ_{P_v}) and available capacity of vehicle v (cap_v^t). This function is proposed as Eq. 4.

$$(c_{rv}, \Lambda_v^t) = PathCost(\Omega_r, \Lambda_v, \Theta_{P_v}, cap_v^t) \quad (4)$$

To solve the proposed single-vehicle DARP problem (adding a new request r to current vehicle path Λ_v), for vehicles which already have at most two scheduled passengers (four locations in their path to pick up/drop off), we enumerate all possible cases to compute the exact optimal path. For vehicles with more than two scheduled passengers, as in [Alonso-Mora et al. \(2017\)](#) and [Simonetto et al. \(2019\)](#), we use an insertion heuristic method (Algorithm 1) based on which new request's pick up and drop off locations are inserted, while the current order of the schedule of Λ_v is kept. For instance, the current travel path of vehicle v is $tour = (+p_2, \underline{p_1}, \underline{p_2})$ which means passenger 2 pick up, passenger 1 drop off, and passenger 2 drop off. Passenger 3 can be added as $newtour = (+\underline{p_3}, p_3, +p_2, p_1, \underline{p_2})$, $newtour = (+p_3, +p_2, \underline{p_1}, \underline{p_2}, \underline{p_3})$, $newtour = (+p_2, \underline{p_1}, +p_3, \underline{p_2}, \underline{p_3})$, and $newtour = (+p_3, +p_2, \underline{p_1}, \underline{p_2}, \underline{p_3})$. The time duration of each $newtour$ is calculated and then the one with minimum travel time is chosen. Given s be the number of scheduled locations (origin and destination) in the vehicle tour, based on the proposed insertion method there would be $(s + 1)$ spots for the new request's origin and destination. Thus, the computational complexity of the insertion method for one request is $O(s^2)$ and for the entire bipartite graph with mk edges is $O(mks^2)$.

Algorithm 1

```

tour  $\leftarrow \Lambda_v$ 
L  $\leftarrow length(tour)$ 
1  $\leftarrow k$ 
tour( $w : y$ ) returns the  $w$ -th index to  $y$ -th index
for  $i=0:L$  do
    newtour  $\leftarrow [tour(1 : i) \ O_r \ tour(i + 1 : end)]$ 
    M  $\leftarrow length(newtour)$ 
    for  $j=i+1:M$  do
        newtour  $\leftarrow [newtour(1 : j) \ D_r \ newtour(j + 1 : end)]$ 
        if newtour satisfies the constraints Z then
             $c_{rv}^k \leftarrow$  time duration of newtour
             $newtour^k \leftarrow newtour$ 
             $k + 1 \leftarrow k$ 
        end if
    end for
end for
 $k^* \leftarrow arg\ min\{c_{rv}^k\}_{k=1,...,maxk}$ 
return  $c_{rv} = c_{rv}^{k^*} \quad \Lambda_v^t = newtour^{k^*}$ 

```

The presented one-to-one matching problem can be mathematically formulated as an integer programming model (5). The decision variable x_{rv} is 1 if vehicle v and request r match with each other and 0 otherwise. The objective function (Eq. 5a) aims at minimizing the total travel time of the vehicles. Constraints 5b and 5c ensure that each vehicle/request is matched with one request/vehicle (if symmetric $|R| = |V|$). Due to the structure of constraints in linear assignment problems which is completely unimodular, the binary constraint $x_{rv} \in \{0, 1\}$ can be relaxed and expressed as Constraint 5d.

$$\begin{aligned}
& \min \sum_{r \in R} \sum_{v \in V} \sum_{(r,v) \in L} c_{rv} x_{rv} & (5a) \\
& \sum_{r \in R: (r,v) \in L} x_{rv} = 1 & \forall v \in V & (5b) \\
& \sum_{v \in V: (r,v) \in L} x_{rv} = 1 & \forall r \in R & (5c) \\
& 0 \leq x_{rv} \leq 1 & (5d)
\end{aligned}$$

To solve the assignment problem 5, we use Hungarian algorithm, which is considered one of the common and effective approaches for such problems.

The output of the one-to-one matching problem here is the matching of requests with vehicles and pick up/drop off scheduling(travel path).

3.4. Step 2: Matching of vehicles

The second step of the algorithm is iterative. In the first iteration, the input is the output of step 1 while for the second iteration or so, the input is the output of the previous iteration. Let $V^t = \{v_1, v_2, \dots, v_n\} \subseteq V$ be the set of assigned vehicles from step 1. P_v^t represents the updated P_v for assigned vehicles which is $P_v^t = R_v - P_v$. R_v for the assigned vehicles in the first iteration is just one request r (as the result of one-to-one matching) while for the next iterations, because vehicles are matched with each other, it may have more requests.

We define a directed graph $G_v = (I^t, L^t)$ where I^t is the set of nodes representing assigned vehicles (V^t) and L^t is the set of directed links. Hereafter in this study graph G_v is called a vehicle graph. A directed link $l_{v,v'}^t \in L^t$ between any two vehicles v and v' ($v, v' \in V^t$) exists if some constraints and criteria set Z^t are satisfied. To create vehicle graph G_v , first we need to determine which nodes can be connected to each other. Fig. 4 showcases an example of the potential nodes that each node can be connected with. Fig. 4a represents a bipartite graph with four requests and seven vehicles. From step 1, we know that each request has a set of feasible vehicles (V_r^f). In Fig. 4b, through one-to-one assignment in step 1, requests and vehicles are matched together. As mentioned, assigned vehicles $V^t = \{v_1, v_4, v_5, v_6\}$ constitute the nodes of vehicle graph (Fig. 4c). Each vehicle $v \in V$ in vehicle graph can only be connected to the set of feasible vehicles of request r (V_r^f). For instance, in vehicle graph in Fig. 4c, v_1 can only be connected to v_4 and v_6 because the set of feasible vehicles of request r_2 in request-vehicle bipartite graph (Fig. 4a) is $V_2^f = \{v_1, v_3, v_4, v_6\}$. Likewise, v_6 can be connected to v_1 and v_5 because r_3 ' feasible vehicle set is $V_3^f = \{v_1, v_3, v_5, v_6\}$. However, v_5 in this vehicle graph as seen cannot be connected to any other vehicle since r_1 ' feasible vehicle set is $V_1^f = \{v_2, v_3, v_5, v_7\}$.

Given the number of assigned vehicles n^t , in the worst case, when each vehicle can be connected to all other vehicles, the complexity is $O(n^{t2})$. However, because from step 1 (3.3) each request is connected to k feasible vehicles, in the worst case, each vehicle can be connected to $(\neq 1)$ vehicles. Thus, the computational complexity is $O(n^t k)$. After determining the feasible nodes for each vehicle graph node, we need to create the set of directed links L^t . To do so, we define some criteria and constraints Z^t : z_1^t) only idle assigned vehicles can be matched with other assigned vehicles (idle/enroute) z_2^t) assigned vehicles with less occupants can be matched with assigned vehicles with more occupants z_3^t) the size of assigned requests set R_v related to assigned vehicle $v \in V^t$ should be less than or equal of current available capacity of other vehicles.

Fig. 5 shows an example to clarify these criteria. Consider vehicle graph in Fig. 5a in which $\{v_1, v_2, v_4\}$ are idle and $\{v_3, v_5\}$ are enroute. It is assumed that the total capacity of vehicles is six, and two vehicles of v_3 and v_5 each has four occupants ($|P_3| = 4$ and $|P_5| = 4$).

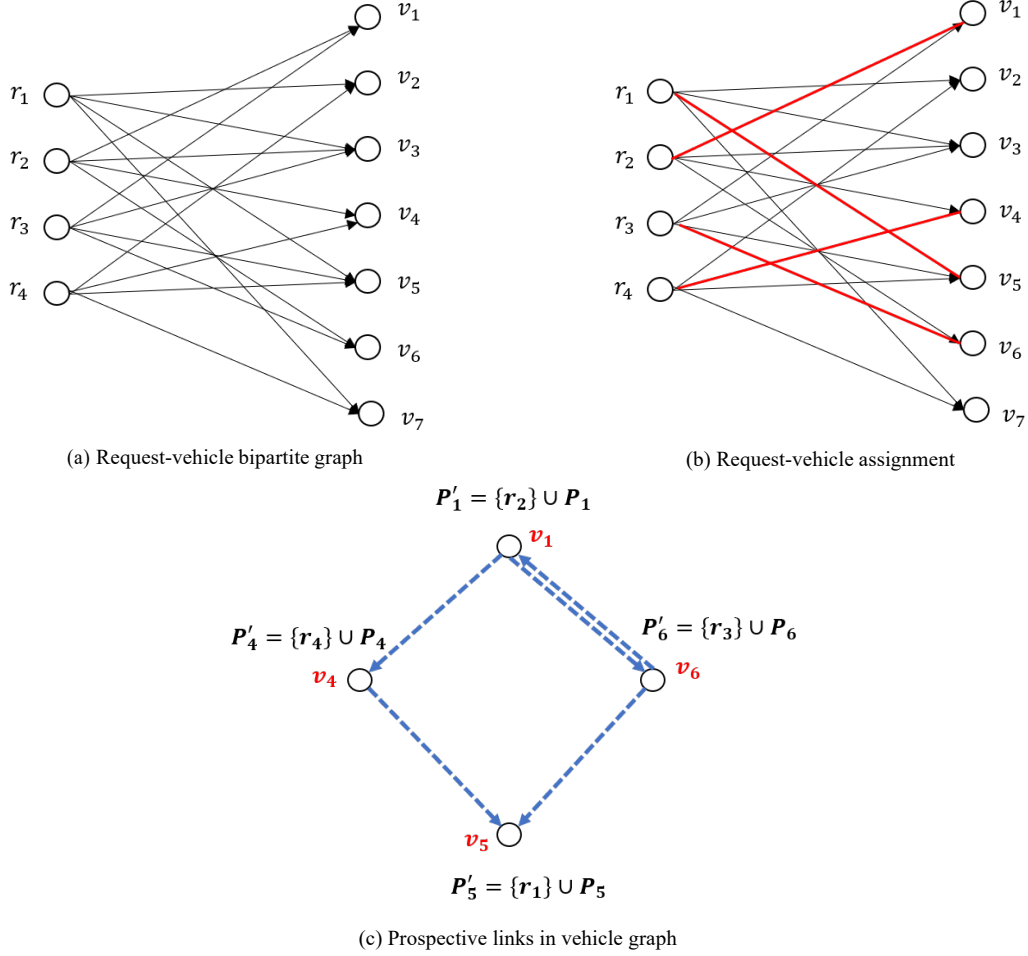


Figure 4: Vehicle graph potential links

Based on the first criteria (z_1^\dagger), idles vehicles $\{v_1, v_2, v_4\}$ can match to any other vehicles while $\{v_3$ and $v_5\}$ as enroute vehicles cannot match. Fig. 5b represents the modified vehicle graph based on z_1^\dagger . Assuming that in the first iteration of step 2, v_2 is matched with v_1 , the vehicle graph in the second iteration is formed as Fig. 5c. In this Figure, based on the second criterion (z_2^\dagger), v_4 can be matched with v_1 ($|P_4^\dagger| = 1 \leq |P_1^\dagger| = 2$), v_1 can be matched with v_3 ($|P_1^\dagger| = 2 \leq |P_3^\dagger| = 5$) and v_4 can be matched with v_5 ($|P_4^\dagger| = 1 \leq |P_5^\dagger| = 5$). The altered vehicle graph can be seen in Fig. 5d. The third criterion (z_3^\dagger) expresses that vehicles should have enough empty space. For instance, in the obtained vehicle graph, shown in Fig. 5e, the set of assigned requests of v_1 ($R_1 = \{r_4, r_3\}$) which has two request members cannot be matched with v_5 because it just has one empty space ($|R_1| = 2 \geq \text{cap}_5^\dagger = 1$) while v_4 can match to other vehicles of v_1 and v_5 .

In addition to these three criteria, constraints $Z = \{z_1, z_2\}$ mentioned in Step 1 need to be satisfied. Notice that constraints should be checked for all members of assigned requests set R_v . As in Step 1, a routing function is used through which these two constraints are checked and optimal path and associated cost is obtained. This routing function is as Eq. 6.

$$(c_{vv}^\dagger, \Lambda^\dagger) = \text{PathCost}(\Omega_{R_v}, \Lambda_v^\dagger, \Theta_{P_v}, \text{cap}_v^\dagger) \quad (6)$$

Where Ω_{R_v} is the spatiotemporal information related to members of assigned requests set (R_v), Λ_v^\dagger is the updated travel path of vehicle v , Θ_{P_v} is the spatiotemporal information of updated scheduled passengers (P_v^\dagger), cap_v^\dagger is the available capacity of vehicle v , c_{vv}^\dagger is the travel cost associated with the directed link (l_{vv}^\dagger) and Λ^\dagger is the optimal travel path of vehicle v^\dagger . To calculate travel cost and optimal travel path, we modified the insertion heuristic method presented in Step 1 (e.g. Algorithm 1) to propose

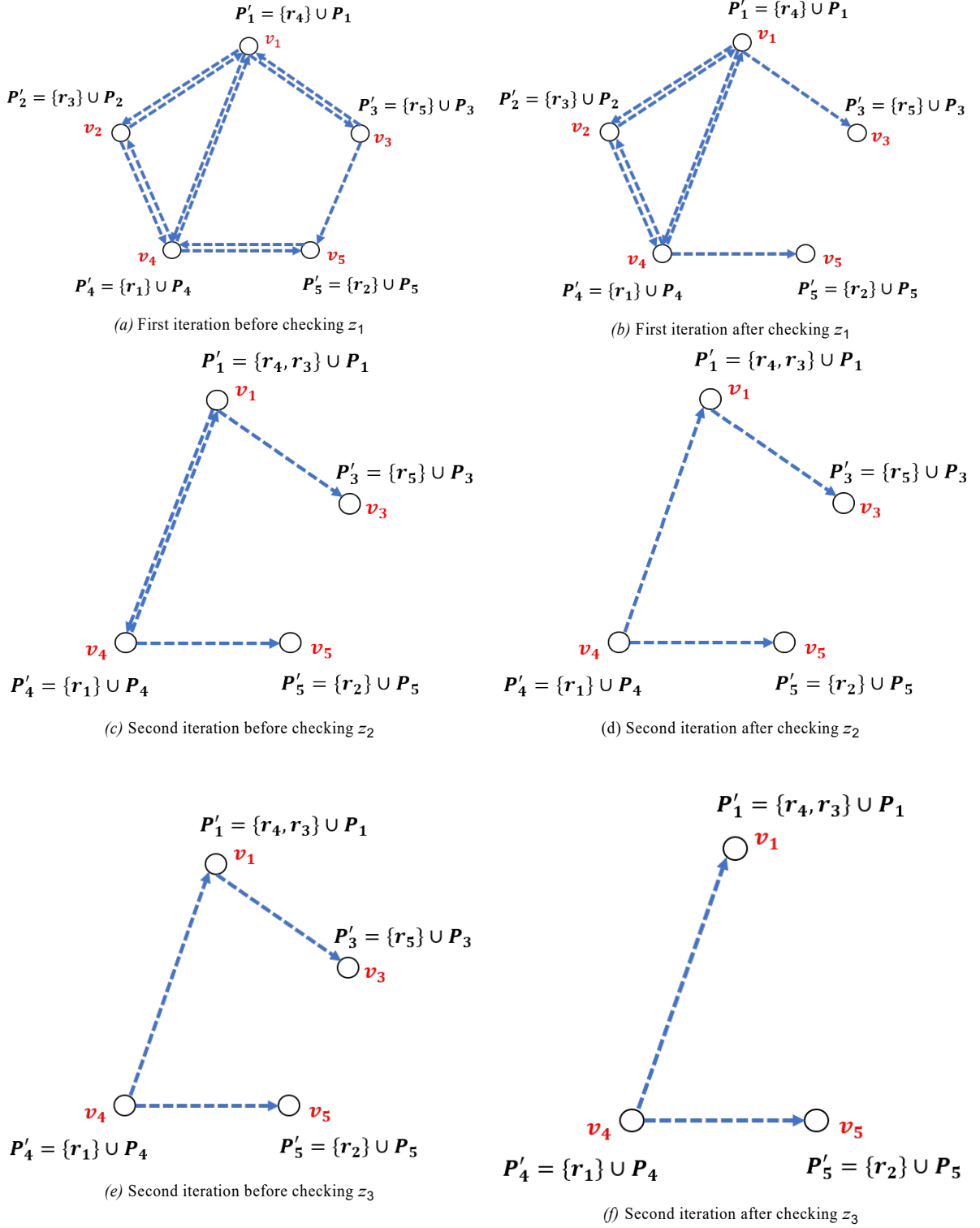


Figure 5: Vehicle graph: creating set of links

algorithm 2.

To illustrate this algorithm, consider two vehicles in Fig. 6 which v_1 is idle and v_2 is enroute. To assign $R_1 = r_1$ to v_2 (e.g. match v_1 to v_2), the current travel path of v_1 , which is represented by $tour = \Lambda_1^t$, is divided into two parts from the middle. To create new a travel path of v_2 , each part is

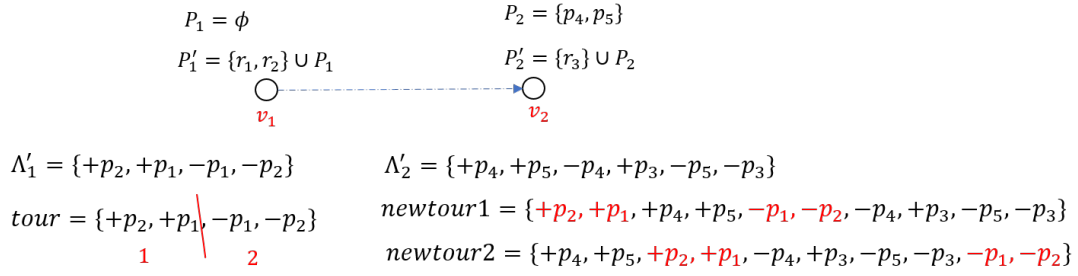


Figure 6: Creating new travel path

added to Λ_2^t , while keeping the current pick up/drop off orders. Notice that to create new path, part 1 of *tour* should be placed before part 2. *newtour1* and *newtour2* in Fig. 6 show two examples of new travel path of v_2 . For each new travel path, the time duration of each *newtour* is calculated and then the one with minimum travel time is chosen. Based on the set of travel costs $c_{vv}^t \in C^t$ acquired from Eq. 6, a set of directed links $l_{vv}^t \in L^t$ of vehicle graph is determined.

Similar to the previous insertion method, given s be the number of scheduled locations in the vehicle tour, there will be $(s + 1)$ spots for the new riders' Part 1 and 2. Thus, the insertion method's computational complexity for one request is $O(s^2)$ and for the entire vehicle graph with $n^t k$ edges is $O(n^t k s^2)$.

Algorithm 2

```

tour1  $\leftarrow \Lambda_v^t$ 
tour breaks into two parts
1stPart  $\leftarrow$  tour first part
2ndPart  $\leftarrow$  tour second part
tour2  $\leftarrow \Lambda_v^t$ 
L  $\leftarrow \text{length}(\text{tour}_2)$ 
Lt  $\leftarrow \text{length}(1\text{stPart})$ 
1  $\leftarrow k$ 
tour( $w : y$ ) returns the  $w$ -th index to  $y$ -th index
for  $i=0:L$  do
  newtour  $\leftarrow [ \text{tour}_2(1 : i) \text{ 1stPart } \text{tour}_2(i + 1 : \text{end}) ]$ 
  M  $\leftarrow \text{length}(\text{newtour})$ 
  for  $j=i+L^t:M$  do
    newtour  $\leftarrow [ \text{newtour}(1 : j) \text{ 2ndPart } \text{newtour}(j + 1 : \text{end}) ]$ 
    if newtour satisfies the constraints Z then
       $c_{vv}^{(k)}$   $\leftarrow$  time duration of newtour
      newtourk  $\leftarrow$  newtour
       $k + 1 \leftarrow k$ 
    end if
  end for
end for
k*  $\leftarrow \arg \min \{ c_{vv}^{(k)} \}$ 
return  $c_{vv}^t = c_{vv}^{(k^*)}$   $\Lambda_v^* = \text{newtour}^{k^*}$ 

```

In the obtained directed vehicle graph, the purpose is to find a match to minimize the total travel cost. To solve this problem, we can convert it into a maximum weight matching problem in a general graph. To do so, travel costs are multiplied by minus one. Also, without the loss of generality, we assume that the vehicle graph is undirected. We can impose this assumption because total weights are independent

from links directions. To solve the maximum weight matching problem, we use Edmonds' algorithm (Saunders, 2013). The computational complexity of this algorithm is $O(|V^t|^3)$, where V^t is the set of assigned vehicles in the vehicle graph.

As Step 2 of the algorithm is iterative, it continues until the set of directed links in vehicle graph is empty ($L^t = \emptyset$). This happens when feasible links are not satisfied criteria or constraints Z^t . The algorithm stops when one of these conditions is satisfied: (1) set of travel requests is empty ($R = \emptyset$), (2) no available vehicles exist, or (3) set of links in bipartite graph G (step 1) is empty ($L = \emptyset$) which happens when constraints Z are not satisfied.

3.5. Computational comparison

In the IBM algorithm Simonetto et al. (2019): (1) context mapping determines the potential vehicles for each request, (2) to specify vehicles travel path, a DARP problem using an insertion heuristic method is used, (3) an integer linear programming to assign requests to vehicles is solved, and (4) a rebalancing strategy for the vehicles is used. In the GMOMatch algorithm, Step 1 includes all stages of the IBM algorithm except for rebalancing. We create a search space to determine the potential vehicles for each request, which is equivalent to the context mapping in IBM with the same computational complexity. To specify the vehicles travel path, we use a heuristic insertion method with the computation complexity of $O(s^2)$ for one request and $O(mks^2)$ for the entire bipartite graph which is a similar complexity as that of IBM. For solving the integer linear programming with N cost matrix, GMOMatch uses Hungarian and IBM uses Auction algorithm—both having the complexity of $O(N^3)$. Unlike the IBM, which does not combine requests, the GMOMatch combines requests in its second step. In Step 2 of the GMOMatch, the computational complexity for the entire vehicle graph is $O(n^tks^2)$ and for solving the maximum weight matching problem in a general graph is $O(V^2.E)$ which V represents number of vertices and E is number of edges. Thus, the computational complexity for the entire algorithm is $O(\max\{mks^2, N^3, n^tks^2, V^2.E\})$, which in the worst case is similar to the IBM algorithm.

4. Case Study and Results

In this section, we briefly introduce the study area and explain how we synthesized the demand. The parameter settings for the simulation of the GMOMatch on micro-traffic simulator are described. To evaluate the performance of the GMOMatch, we compare it with the IBM algorithm and discuss on the obtained results. Finally, to assess how changing various variables and GMOMatch parameters affect the performance of the algorithm, a detailed sensitivity analysis is conducted.

4.1. Case Study Implementation

We considered road network of Downtown Toronto as the study area. One of the reasons for choosing this network is that it faces recurrent congestion during morning and afternoon peak periods. Fig. 7 presents the network (3.14km x 3.31km), which consists of 268 nodes/intersections and 839 links.

We implemented the GMOMatch algorithm and the road network of Downtown Toronto in MATLAB and applied them on an in-house agent-based micro-traffic simulator (Djavadian and Farooq, 2018). The dynamic demand loading period in this study was 7:45am-8:00am (15 minutes) in the morning peak period. The demand used in this study is time-dependent exogenous Origin-Destination (OD) demand matrices for the year 2018, which is based on 5 minutes intervals and were obtained from the Transportation Tomorrow Survey (TTS) of Toronto. The demand within 5 minutes were distributed randomly using a Poisson distribution. From the total demand of 5,487 trips in the loading period, we randomly extracted a percentage (e.g. 10%, 15%, 20%, 25%), as the shared vehicles demand, while the rest of the demand was assumed to travel by their own single occupancy private vehicles. In this study, we did not have any fleet size optimization and the size was set exogenously.

Although the network loading time was 15 minutes, the simulation time lasted until all passengers either arrived at their destination or left the system. It was assumed that link-level space mean speed can be monitored, which was used by the routing agent to provide dynamic travel-time based shortest paths. The assumption is based on the fact that downtown Toronto already has enough sensors installed

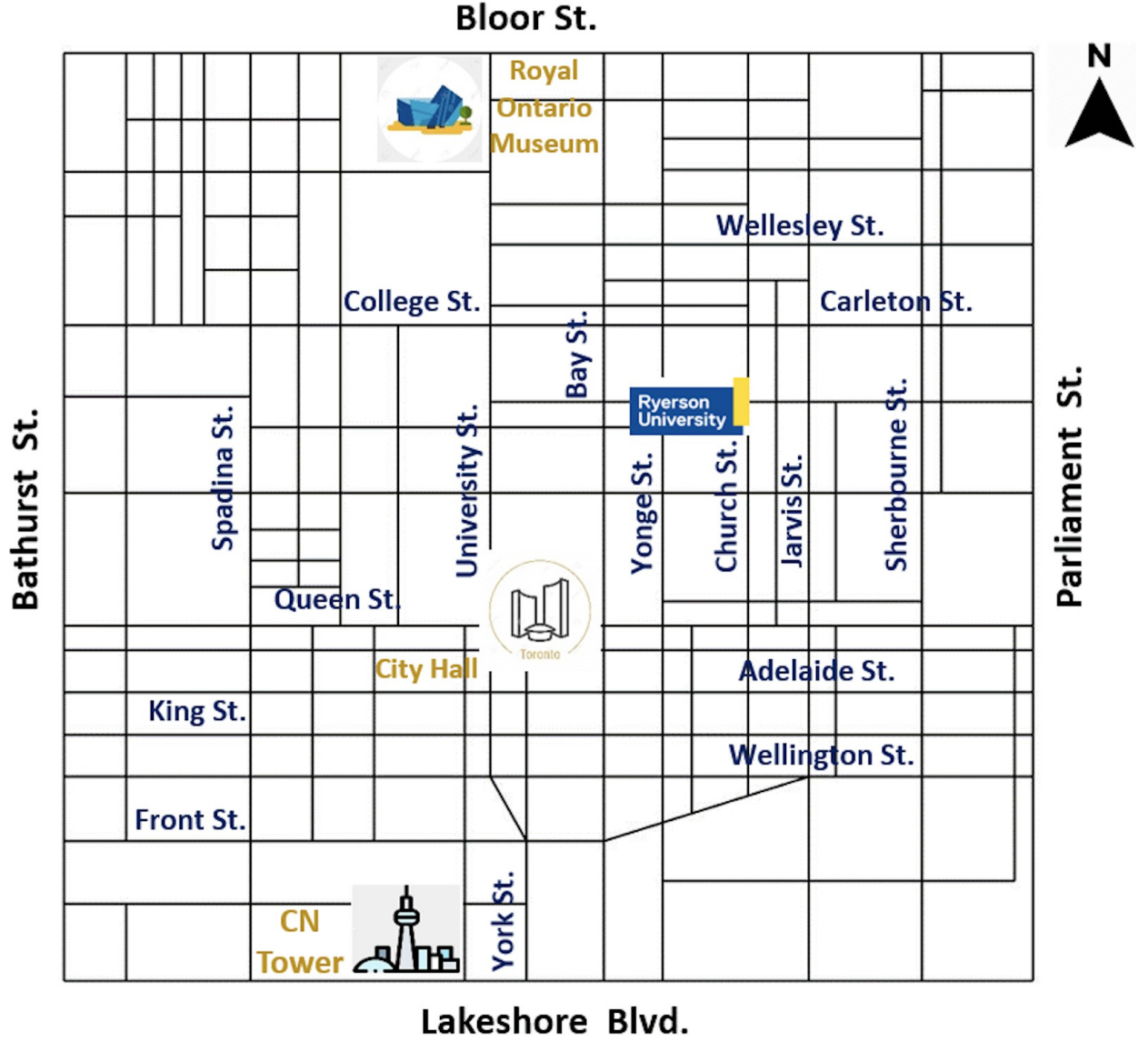


Figure 7: Downtown Toronto street network

that can provide a quasi-real-time state of the network. We assumed that the riders left the system after their latest departure time, if they were not assigned to any vehicles. Also, as mentioned in Section 3.1, to make the ride-matching system more dynamic we assumed that the travel request time equals earliest the departure time ($t_r = e_r$).

To evaluate the performance of our GMOMatch algorithm, we compared the results with a ride-matching algorithm developed by [Simonetto et al. \(2019\)](#) (called IBM algorithm in this paper), which is an algorithm based on the linear assignment problem. We chose this algorithm because in terms of computational complexity it is one of the best algorithms in the literature, while it maintains the quality of the service. Also, unlike other recent studies that used partitioning or decomposition methods ([Masoud and Jayakrishnan, 2017a](#); [Tafreshian and Masoud, 2020](#)), IBM algorithm, like GMOMatch, is formulated centrally and has the full view of the network. For the sake of comparison, we implemented the IBM algorithm in MATLAB and applied it on the micro-traffic simulator. In both GMOMatch and IBM algorithms, the shared vehicles are distributed proportional to the ridesharing demand such that locations with more demand have more shared vehicles. It is worth mentioning that the IBM algorithm in [Simonetto et al. \(2019\)](#), required rebalancing vehicles, while the GMOMatch can perform at high level without it. All simulations were implemented on three computers, including two computers with Core i7-8700 CPU, 3.20 GHz Intel with a 64-bit version of the Windows 10 operating system with 16.0 GB

RAM and one computer with Core i7-6700K CPU, 4.00 GHz Intel with a 64-bit version of the Windows 10 operating system with 16.0 GB RAM.

4.2. Results

The first part of this section is related to comparing the performance of GMOMatch with IBM, and in the second part, a detailed sensitivity analysis is conducted to show the impact of different parameters on the quality of indicators. We considered eight indicators to measure for both algorithms. Table 2 shows the indicators with the abbreviations and their descriptions.

Table 2: Indicators, their abbreviations and descriptions

| Indicators | Abbreviation | Description |
|---|--------------|---|
| Service rate (%) | SR | The percent of served requests per total requests |
| Average vehicle km traveled | VKT | Km traveled by each shared vehicle |
| Average detour time (min) | DT | The difference between shared ride travel time and direct travel time for a new request |
| Average wait time (min) | WT | The difference between new rider's pick up time and request time |
| Average traffic travel time (min) | TTT | Average all vehicles' travel time |
| Average traffic speed (km/hr) | TS | Average all vehicles' speed |
| Average number of assignments | No. A | Average number of request assignment per shared vehicle over the simulation period |
| Average computation time per call (sec) | - | Average time it takes the algorithm is solved at each update time |

To compare the performance of GMOMatch with IBM, we created five scenarios by varying the fleet size (210, 230, 250, 270, 290). The shared vehicles demand is considered to be 25% of the total demand, which came out to be 1,372 trips. The flexibility was assumed to be five minutes ($f = 5min$), vehicle capacity was four ($cap = 4$), and the update interval $\Delta = 30sec$. Fig. 8 compares the performance of the GMOMatch with IBM over different parameters. It is worth mentioning that the simulation run-time for each scenario was between 30 and 36 hours.

Fig. 8a shows the service rate (SR) for the two algorithms. For different fleet sizes, the GMOMatch yields better service rate, compared to the IBM. For the fleet size of 290, service rate for the GMOMatch was 95.39%, while for IBM this number was 72.13%, which shows a 32% improvement. One of the reasons for such a large difference is that IBM algorithm is based on one-to-one matching, which means that at each update time only one new request can be assigned to a vehicle despite the existence of some requests with similar itineraries at one location. Fig. 8a shows that this feature affects the service rate negatively, because in congested networks the probability of having several requests with similar itineraries is high, especially with specific origins/destinations such as first-mile or last-mile problems. In contrast, the GMOMatch by combining requests with the same number of vehicles and without any rebalancing, increased the service rate, indicating the high performance of the algorithm. To have a better comparison between the two algorithms, in the other figures, besides the main indicator, we include service rate on the right-side of the graphs.

Fig. 8b shows the average VKT of shared vehicles over the simulation period. The GMOMatch showed lower values of VKT than the IBM. As an example, for the fleet size of 290, the GMOMatch showed 16.07% improvement when compared to the IBM, while its service rate was 32% higher. One of the reasons is that in the IBM, because of one-to-one matching the vehicles that are enroute have to change their travel path more frequently and sometimes they may take longer path to pick up new passengers. This repetitive change in their travel path leads to increase in VKT. However, in the GMOMatch vehicles are usually assigned multiple passengers instead of one. This results in having less change in the travel path and decrease in VKT. Fig. 8c and Fig. 8d demonstrate the average wait time (WT) and average detour time (DT) for different fleet sizes. Here there are no significant differences between the two algorithms. However, it is noticed that the GMOMatch with similar detour time and wait time as IBM served much higher number of requests.

Fig. 8e and Fig. 8f represent the average traffic travel time (TTT) and average traffic speed (TS) in the network. In Fig. 8e, average traffic travel time for the GMOMatch over different scenarios yielded better results such that for the fleet size of 290, it showed 4.26% reduction when compared to IBM. Also, the average traffic speed in Fig. 8f, for all scenarios in the GMOMatch showed higher speed values such

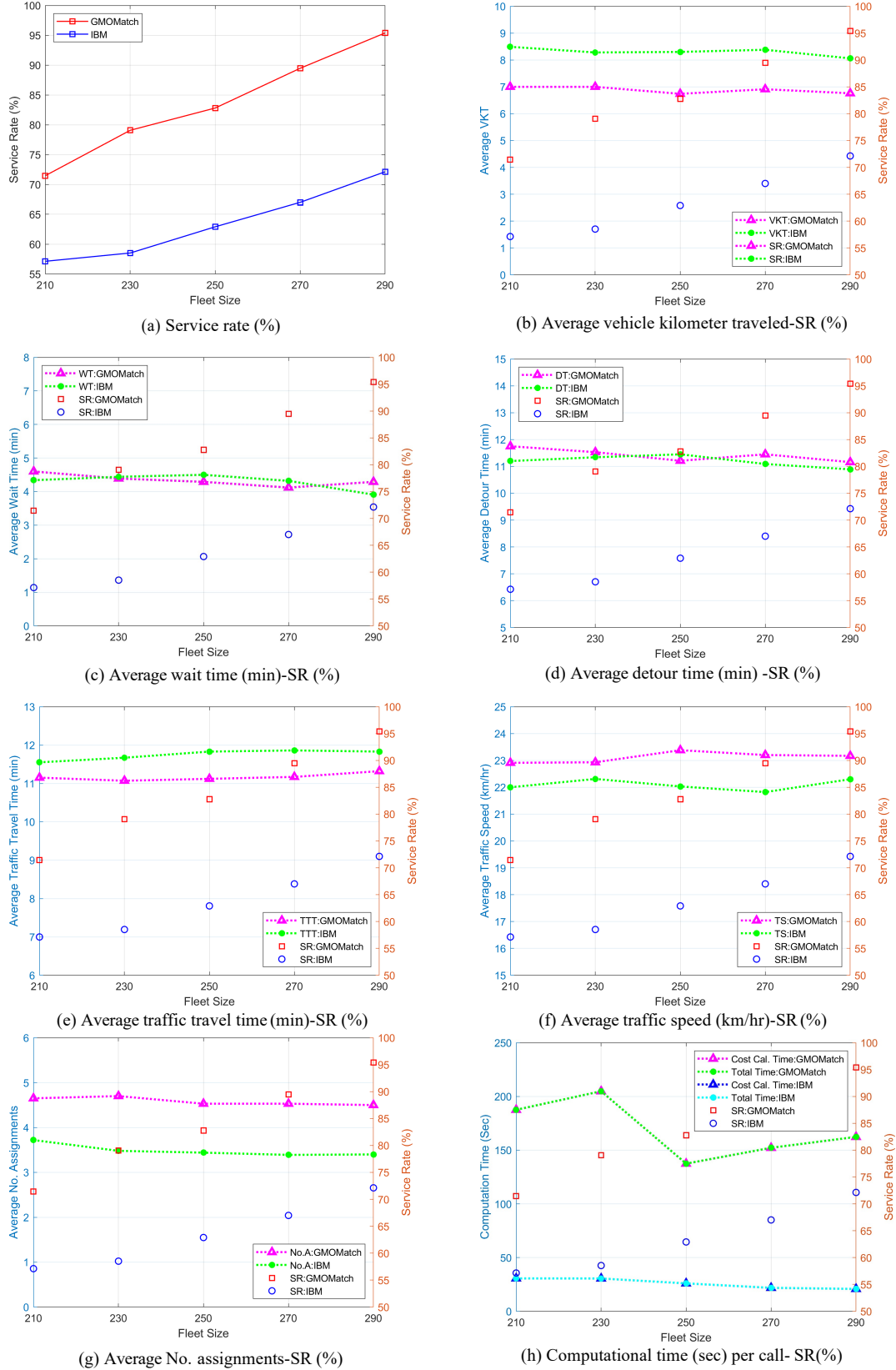


Figure 8: Different parameters vs fleet size: demand=25%, $f=5\text{min}$, $\text{cap}=4$, $\Delta = 30\text{sec}$

that there was a 4.07% increase for the fleet size of 290. The reason is that the IBM algorithm increases the number of shared vehicles in the road network because at each update time some idle shared vehicles

may be assigned to new requests. These idle vehicles, which have only one occupant when they start traveling, enter the road network and worsen the traffic congestion. However, combining requests in the GMOMatch increases the vehicle occupancy rate and reduces the number of shared vehicles on the road network. This leads to improvement in traffic travel time and traffic speed. These improvements are accompanied with a higher service rate for the GMOMatch.

Fig. 8g shows the average number of assignments per vehicle during the simulation period. As shown in the figure, the average number of assignments per vehicle for the GMOMatch for different fleet size is higher than the IBM. As discussed earlier, combining requests in the GMOMatch in comparison with the one-to-one matching in the IBM improves the system's efficiency because in the congested networks the probability of having several requests with similar itineraries is high. Thus, at each update time a vehicle in the GMOMatch algorithm may become fully-occupied, while in the IBM just one request is assigned to the vehicle. In the IBM algorithm because of one-to-one matching, it takes more time for the vehicle to become fully-occupied.

Fig. 8h shows the average computational time per request for two algorithms. The computational time consists of two components: cost calculation time and total time. The cost calculation time for the GMOMatch includes creating bipartite graph along with solving insertion method in Step 1, and creating vehicle graph plus solving insertion method in Step 2. Total time is the summation of cost calculation time and solution time. Solution time represents the time it takes to solve one-to-one matching problem in Step 1 and maximum weight matching problem in Step 2. Most of the computational time portion is related to the cost calculation time in both algorithms. Although the IBM algorithm reports less computational time than the GMOMatch, its service rate yields much lower values. It is worth mentioning that all of the cost calculations and travel times are computed on-line and there are no precomputed travel times. Using precomputed/predicted travel time, or computing travel time with less frequencies (e.g. every three minutes instead of every one minute) can significantly reduce the computation time. Also, most of the calculations for creating bipartite graph in Step 1, vehicle graph in Step 2, and solving the insertion method can be computed in parallel, which would decrease the cost computational time remarkably.

In the second part of the results, we conducted a detailed sensitivity analysis. Table 3 reports the results obtained by running simulations over different variables and significant algorithm parameters. Three scenarios were created by varying demand, fleet size, vehicle capacity, and flexibility to explore how changing the different parameters affect the system performance.

In the first scenario, we considered four various demand percentages, including 10%, 15%, 20%, and 25% with 150 vehicles, while keeping the other parameters constant. With the 10% demand and 150 vehicle, service rate was 100% and all of the riders are served. As expected, by increasing the demand, service rate reduced significantly such that with 25% demand, this number was 58.89%. It is observed that the growth in demand resulted in the increase of the vehicles kilometer traveled. Whereas, the growth had decreased the detour time as well as the waiting time. In the former, although service rate decreases, vehicles serve more riders during the simulation period, thus, more VKT was observed. However, in the latter, with the growth of demand the probability of finding a better match increases. A better match means riders with similar itineraries are grouped and assigned to a vehicle which can lead to reduction in waiting time and detour time. Finding a better match and lower values of detour time can mitigate traffic congestion because vehicles do not have to take long distance to pick up/drop off passengers. As a result, vehicles may have less change in their travel path and fewer lane changing when traveling through the road network which means lower interruption in the traffic flow and enhancement in traffic travel time and traffic speed. By increasing the demand, both cost calculation time and solution time increased. This was because the number of iterations in the GMOMatch increased, including the main iterations and iterations related to Step 2. When the demand increased, while the fleet size was fixed, the number of new requests might have exceeded the number of available vehicles. Since step 1 of the GMOMatch is one-to-one matching, the maximum number of requests that can be assigned equals the number of available vehicles. Thus, the algorithm had to move toward next iterations to match the remaining requests. Thus, both cost calculation time and solution time increased.

In the second scenario in Table 3, we used 25% demand, that remained fixed for all the instances. We

considered three fleet sizes of 210, 230, and 250. For each fleet size, we tested three capacities of 4, 6, and 10. For each fleet size, with the increase in the capacity, service rate increased. The service rate was 100% for the capacity of 10, for all the fleet sizes. In a congested network with high shared vehicles demand, there might be many requests whose origins and destinations are close to each other. Therefore, they can be combined and assigned to one vehicle. This indicates the efficiency of using medium/high-capacity vehicles in the congested areas where there are enough requests with similar itineraries. [Sanaullah et al. \(2021\)](#) also came to a similar conclusion after evaluating the on-demand public transit in Belleville, Canada.

Table 3: Results for different values of demand, fleet size, flexibility, and capacity

| Scenarios | Fleet Size | Demand (%) | f (min) | Δ (sec) | cap | SR (%) | VKT | Detour (min) | Waiting (min) | Traffic Travel Time (min) | Traffic Speed (km/hr) | Cost Time (s) | Solution Time (s) |
|-----------|------------|------------|---------|----------------|-----|--------|-------|--------------|---------------|---------------------------|-----------------------|---------------|-------------------|
| 1 | 150 | 10 | 5 | 60 | 6 | 100.00 | 6.51 | 13.54 | 4.69 | 12.57 | 21.48 | 283 | 0.135 |
| | 150 | 15 | 5 | 60 | 6 | 89.16 | 6.72 | 11.90 | 4.56 | 11.96 | 22.41 | 451 | 0.214 |
| | 150 | 20 | 5 | 60 | 6 | 69.93 | 7.27 | 12.16 | 4.56 | 11.34 | 22.45 | 786 | 0.245 |
| | 150 | 25 | 5 | 60 | 6 | 58.89 | 7.46 | 11.14 | 4.21 | 10.84 | 23.20 | 963 | 0.302 |
| 2 | 210 | 25 | 5 | 60 | 4 | 79.44 | 6.70 | 10.25 | 3.61 | 11.05 | 23.18 | 538 | 0.140 |
| | 210 | 25 | 5 | 60 | 6 | 82.30 | 7.15 | 11.24 | 4.35 | 11.16 | 23.15 | 652 | 0.247 |
| | 210 | 25 | 5 | 60 | 10 | 100.00 | 6.66 | 11.47 | 4.22 | 10.79 | 23.52 | 1224 | 0.328 |
| | 230 | 25 | 5 | 60 | 4 | 85.52 | 6.54 | 10.24 | 3.52 | 11.19 | 23.05 | 523 | 0.133 |
| | 230 | 25 | 5 | 60 | 6 | 90.78 | 7.26 | 11.33 | 4.18 | 11.14 | 22.98 | 570 | 0.178 |
| | 230 | 25 | 5 | 60 | 10 | 100.00 | 6.67 | 12.02 | 4.35 | 10.82 | 23.19 | 1028 | 0.353 |
| | 250 | 25 | 5 | 60 | 4 | 91.88 | 6.47 | 10.38 | 3.47 | 11.31 | 22.67 | 416 | 0.487 |
| | 250 | 25 | 5 | 60 | 6 | 95.17 | 6.96 | 11.40 | 4.21 | 11.20 | 22.89 | 475 | 0.143 |
| | 250 | 25 | 5 | 60 | 10 | 100.00 | 6.53 | 11.68 | 4.29 | 10.92 | 23.22 | 1207 | 0.329 |
| | 170 | 25 | 5 | 60 | 6 | 70.30 | 7.50 | 11.15 | 4.16 | 11.04 | 23.36 | 764 | 0.316 |
| | 170 | 25 | 10 | 60 | 6 | 76.37 | 10.32 | 14.06 | 7.08 | 10.74 | 23.05 | 1017 | 0.173 |
| | 190 | 25 | 5 | 60 | 6 | 75.05 | 7.22 | 11.35 | 4.20 | 10.95 | 22.84 | 690 | 0.286 |
| 3 | 190 | 25 | 10 | 60 | 6 | 84.86 | 10.29 | 14.38 | 7.32 | 10.99 | 22.67 | 1127 | 0.186 |
| | 210 | 25 | 5 | 60 | 6 | 82.30 | 7.15 | 11.24 | 4.35 | 11.16 | 23.15 | 652 | 0.247 |
| | 210 | 25 | 10 | 60 | 6 | 94.22 | 10.21 | 14.09 | 6.96 | 10.96 | 23.10 | 911 | 0.234 |
| | 230 | 25 | 5 | 60 | 6 | 90.78 | 7.26 | 11.33 | 4.18 | 11.14 | 22.98 | 570 | 0.178 |
| | 230 | 25 | 10 | 60 | 6 | 100.00 | 10.25 | 13.93 | 7.19 | 11.05 | 22.65 | 910 | 0.221 |
| | | | | | | | | | | | | | |

For each fleet size, VKT, detour time and waiting time increased when the capacity increased from 4 to 6. One of the reasons is that for the capacity of 6 when the vehicles are enroute and have one or two empty spaces, they may be assigned new riders, which could lead to the rise in VKT, detour time, and waiting time. For vehicles with the capacity of 10, VKT had lower values when compared to the capacity of 6, while detour time and waiting time for the fleet of 230 and 250 showed slightly higher values. Traffic travel time and traffic speed for vehicles with capacity of 10, for all three fleet sizes, showed better values when compared to the capacity of 4 and 6. One of the reasons is that vehicles with capacity of 10 can transport more passengers at a time. Thus, their operational time over the simulation period might be less than vehicles with the capacity of 6 and 4. This led to a fewer number of shared vehicles on the road network, improving the traffic travel time and traffic speed. Both indicators related to the computational time for all the fleet sizes, showed an increase when using vehicles with higher capacity. One of the reasons is that using vehicles with more capacity may increase the number of iterations in Step 2 of the algorithm. This is because more empty seats were available for the vehicles

and more vehicle matching and consequently more requests combining may occur. However, there was a significant difference between vehicles with capacity of 10 and the other two capacity options. Such a significant difference indicates that using high-capacity vehicles despite improving the service quality is computationally expensive, especially when the shared vehicles demand is high.

In the third scenario, the demand was 25%, and we considered four fleet sizes, including 170, 190, 210, and 230. For each fleet size, we tested two flexibility levels (i.e., 5 and 10 minutes). For $f = 10$, the service rate was higher for all fleet sizes. It is because riders keep staying in the ride-matching system 5 more minutes. During these 5 more minutes, some vehicles would become available and can be assigned to the riders. As a result of serving more riders, the VKT increased for different fleet sizes compare to $f = 5$. Also the detour time and waiting time reported higher values for $f = 10$, for all the fleet sizes. This is because the riders had to wait more to be assigned and picked up. For higher detour time, one of the reasons was that the itineraries for riders who had not been assigned are less similar to each other, which may lead to rise in detour time. The increase in flexibility did not have any significant effect on the traffic travel time and traffic speed. Both cost calculation time and solution time increased for $f = 10$. As reported for the cost calculation time, there was a significant difference between the two flexibility options. This was because by increasing the flexibility, at each update time, there are new requests and many unmatched requests from previous update times. Hence, the number of requests was higher than the number of vehicles. As discussed earlier, this increased the number of main iterations of the algorithm, which can result in an increase in the cost calculation time.

5. Conclusion and future directions

We developed a novel Graph-based Many-to-One ride-Matching (GMOMatch) algorithm for solving the dynamic many-to-one ride-matching problem for shared on-demand mobility services in congested urban networks. The algorithm is iterative and has two steps. It starts by creating a bipartite graph and solves a one-to-one ride-matching problem. In the second step, a vehicle directed graph is developed and solved using the maximum weight matching problem to match the vehicles and combine the associated requests. To evaluate the performance of our algorithm, we compared it with a ride-matching algorithm developed by [Simonetto et al. \(2019\)](#) at IBM, which is based on the linear assignment problem. We implemented two algorithms on an in-house micro-traffic simulator to compare their performance in the presence of traffic congestion. Downtown Toronto road network was used as the case study.

The results of the study demonstrated that GMOMatch improved the service rate by 32% when compared to the IBM algorithm with 290 vehicles of capacity 4. Along with a higher service rate, it showed either enhancement or similar performance for other indicators. VKT and number of assignments per vehicle showed 16.07% and 32% improvement, respectively. Although there were no significant differences for the wait time and detour time between two algorithms, the GMOMatch served more requests than the IBM algorithm. Comparing two algorithms also revealed that the GMOMatch alleviated the traffic congestion by increasing the average traffic speed (4.07%) and reducing the average traffic travel time (4.26%) of the traffic on the network. Overall, the GMOMatch algorithm ameliorated both service quality and traffic congestion, while its computational complexity was the same as that of IBM. To further examine the performance of GMOMatch, a detailed sensitivity analysis was performed over various parameters, including demand, fleet size, flexibility, and vehicle capacity. The sensitivity analysis showed that increasing the vehicle capacity from 4 to 10 with 210 vehicles in the congested network resulted in a 100% service rate, which is a 25% improvement. Although, some slight increase in the detour time and waiting time was observed, there was an improvement in other indicators, including VKT, traffic travel time and traffic speed. The use of higher capacity vehicles led to a more efficient utilization of the supply and operation of lower fleet size on the network. Our results showed that by increasing the demand and keeping the fleet size fixed, the service rate reduced. However, some indicators such as detour time, traffic speed, and traffic travel time showed an improvement of 1%, 4%, and 4%, respectively. This indicates that in case of having enough demand, the operator can more likely find riders with similar origin-destinations and use the vehicle capacity better. We expect that this work will be useful for the design and operations of on demand shared mobility services using medium/high capacity vehicles in

dense urban areas, where congestion is a recurrent issue. Furthermore, the proposed algorithm could be useful for the first mile/last mile service for freight or passenger systems, where an origin or destination is fixed.

In less congested areas, combining the requests may increase the VKT, wait time and detour time. The probability of finding requests with similar itineraries is lower, either when the rate of the shared vehicles demand is low or when the update time interval to run the matching algorithm is very short. One of the ways to address these limitations is to develop a reinforcement learning system that can dynamically assess the need of Step 2 in GMOMatch, based on the changing spatiotemporal dynamics of demand. This way, only the one-to-one matching problem in Step 1 is run iteratively and the operator can consistently keep the service quality at high level.

All of the cost computations in this study have been calculated centrally. In the future, distributed computing and different graph partitioning methods can be used to reduce the cost calculation time. A promising option to use here is the distributed system designed by Farooq and Djavadian (2019). Such distributed systems can significantly decrease the computational time by only performing local level computations. As mentioned, our data in this study were generated from a simulation. Having access to the real data can give better insights into user behaviour, which would be helpful for adjusting the algorithm parameters to improve the efficiency of the ride-matching system. Combining the two steps of the proposed algorithm can be explored using the k-partite matching approaches suggested by Anderson and Farooq (2017). The proposed ride-matching algorithm in this study does not have any vehicle relocation, inclusion of which can further improve the performance. Predicting demand and developing a vehicle relocation system using machine learning techniques can significantly enhance the service quality.

Acknowledgement

This research is partially funded by the Canadian Urban Transit Research and Innovation Consortium. We would like to thank Dr. Shadi Djavadian for implementing the base traffic micro-simulator that was adapted in this study and for providing advice on the developing the Downtown Toronto roadway network used in this study as well as on the implementation of our ride-matching algorithms in the micro-simulator.

References

- N. Agatz, A. L. Erera, M. W. Savelsbergh, and X. Wang. Dynamic ride-sharing: A simulation study in metro atlanta. *Procedia-Social and Behavioral Sciences*, 17:532–550, 2011.
- N. Agatz, A. Erera, M. Savelsbergh, and X. Wang. Optimization for dynamic ride-sharing: A review. *European Journal of Operational Research*, 223(2):295–303, 2012.
- J. Alonso-Mora, S. Samaranayake, A. Wallar, E. Frazzoli, and D. Rus. On-demand high-capacity ride-sharing via dynamic trip-vehicle assignment. *Proceedings of the National Academy of Sciences*, 114(3):462–467, 2017.
- P. Anderson and B. Farooq. A generalized partite-graph method for transportation data association. *Transportation Research Part C: Emerging Technologies*, 76:150–169, 2017.
- D. Bertsimas, P. Jaillet, and S. Martin. Online vehicle routing: The edge of optimization in large-scale applications. *Operations Research*, 67(1):143–162, 2019.
- J. Castiglione, D. Cooper, B. Sana, D. Tischler, T. Chang, G. D. Erhardt, S. Roy, M. Chen, and A. Mucci. Tncs & congestion. 2018.
- F. Dandl, B. Bracher, and K. Bogenberger. Microsimulation of an autonomous taxi-system in munich. In *2017 5th IEEE International Conference on Models and Technologies for Intelligent Transportation Systems (MT-ITS)*, pages 833–838. IEEE, 2017.
- S. Djavadian and B. Farooq. Distributed dynamic routing using network of intelligent intersections. In *ITS Canada Annual General Meeting Conference, Niagara Falls*, 2018.
- B. Farooq and S. Djavadian. Distributed traffic management system with dynamic end-to-end routing, 2019. URL <https://patentscope.wipo.int/search/en/detail.jsf?docId=WO2020257926>. U.S. provisional patent 62/865,725.
- G. Feng, G. Kong, and Z. Wang. We are on the way: Analysis of on-demand ride-hailing systems. *Available at SSRN 2960991*, 2017.

- M. Guériau, F. Cugurullo, R. Acheampong, and I. Dusparic. Shared autonomous mobility-on-demand: Learning-based approach and its performance in the presence of traffic congestion. *IEEE Intelligent Transportation Systems Magazine*, 2020.
- L. Häme. An adaptive insertion algorithm for the single-vehicle dial-a-ride problem with narrow time windows. *European Journal of Operational Research*, 209(1):11–22, 2011.
- S. C. Ho, W. Y. Szeto, Y.-H. Kuo, J. M. Leung, M. Petering, and T. W. Tou. A survey of dial-a-ride problems: Literature review and recent developments. *Transportation Research Part B: Methodological*, 111:395–421, 2018.
- Y. Huang, K. M. Kockelman, V. Garikapati, L. Zhu, and S. Young. Use of shared automated vehicles for first-mile last-mile service: Micro-simulation of rail-transit connections in austin, texas. *Transportation Research Record*, page 0361198120962491, 2020.
- J. Jung, R. Jayakrishnan, and J. Y. Park. Dynamic shared-taxi dispatch algorithm with hybrid-simulated annealing. *Computer-Aided Civil and Infrastructure Engineering*, 31(4):275–291, 2016.
- M. Liu, Z. Luo, and A. Lim. A branch-and-cut algorithm for a realistic dial-a-ride problem. *Transportation Research Part B: Methodological*, 81:267–288, 2015.
- M. Lokhandwala and H. Cai. Dynamic ride sharing using traditional taxis and shared autonomous taxis: A case study of nyc. *Transportation Research Part C: Emerging Technologies*, 97:45–60, 2018.
- G. Lyu, W. C. Cheung, C.-P. Teo, and H. Wang. Multi-objective online ride-matching. *Available at SSRN 3356823*, 2019.
- N. Masoud and R. Jayakrishnan. A decomposition algorithm to solve the multi-hop peer-to-peer ride-matching problem. *Transportation Research Part B: Methodological*, 99:1–29, 2017a.
- N. Masoud and R. Jayakrishnan. A real-time algorithm to solve the peer-to-peer ride-matching problem in a flexible ridesharing system. *Transportation Research Part B: Methodological*, 106:218–236, 2017b.
- A. Mourad, J. Puchinger, and C. Chu. A survey of models and algorithms for optimizing shared mobility. *Transportation Research Part B: Methodological*, 2019.
- A. Najmi, D. Rey, and T. H. Rashidi. Novel dynamic formulations for real-time ride-sharing systems. *Transportation research part E: logistics and transportation review*, 108:122–140, 2017.
- M. Nourinejad and M. J. Roorda. Agent based model for dynamic ridesharing. *Transportation Research Part C: Emerging Technologies*, 64:117–132, 2016.
- S. Oh, R. Seshadri, D.-T. Le, P. C. Zegras, and M. E. Ben-Akiva. Evaluating automated demand responsive transit using microsimulation. *IEEE Access*, 8:82551–82561, 2020.
- E. Özkan and A. R. Ward. Dynamic matching for real-time ride sharing. *Stochastic Systems*, 10(1):29–70, 2020.
- X. Qian, W. Zhang, S. V. Ukkusuri, and C. Yang. Optimal assignment and incentive design in the taxi group ride problem. *Transportation Research Part B: Methodological*, 103:208–226, 2017.
- H. Ritchie. Urbanization. *Our World in Data*, 2018. <https://ourworldindata.org/urbanization>.
- I. e. c. Sanaullah, N. e. c. Alsaleh, S. Djavadian, and B. Farooq. Spatio-temporal analysis of on demand transit: A case study of belleville, canada. *Transportation Research Part A: Policy and Practice*, 145:284–301, 2021.
- Saunders. Weighted maximum matching in general graphs - file exchange - matlab central. <https://www.mathworks.com/matlabcentral/fileexchange/42827-weighted-maximum-matching-in-general-graphs>, 2013. (Accessed on 12/03/2020).
- M. W. Savelsbergh and M. Sol. The general pickup and delivery problem. *Transportation science*, 29(1):17–29, 1995.
- S. Shaheen, A. Cohen, M. Randolph, E. Farrar, R. Davis, and A. Nichols. Shared mobility policy playbook. 2019.
- A. Simonetto, J. Monteil, and C. Gambella. Real-time city-scale ridesharing via linear assignment problems. *Transportation Research Part C: Emerging Technologies*, 101:208–232, 2019.
- A. Tafreshian and N. Masoud. Trip-based graph partitioning in dynamic ridesharing. *Transportation Research Part C: Emerging Technologies*, 114:532–553, 2020.
- A. Tafreshian, N. Masoud, and Y. Yin. Frontiers in service science: Ride matching for peer-to-peer ride sharing: A review and future directions. *Service Science*, 12(2-3):44–60, 2020.
- H. Wang and H. Yang. Ridesourcing systems: A framework and review. *Transportation Research Part B: Methodological*, 129:122–155, 2019.
- H. Yu, X. Jia, H. Zhang, X. Yu, and J. Shu. Psride: Privacy-preserving shared ride matching for online ride hailing systems. *IEEE Transactions on Dependable and Secure Computing*, 2019.